Hindawi
Advances in Civil Engineering
Volume 2018, Article ID 5804051, 12 pages
https://doi.org/10.1155/2018/5804051

Research Article

Impact of High-Rise Buildings Construction Process on Adjacent Tunnels

Haifeng Guo, Aijun Yao, Jiantao Zhang, Yijun Zhou, and Yanfei Guo

College of Architecture and Engineering, Institute of Geotechnical and Underground Engineering, Beijing University of Technology, Beijing 100124, China

Correspondence should be addressed to Haifeng Guo; ghf_doudou@sina.com

Received 22 January 2018; Revised 30 May 2018; Accepted 24 June 2018; Published 26 July 2018

Academic Editor: Dong-Sheng Jeng

The demand for buildings constructed along subway lines is increasing, and analysis of the impact of foundation excavation and building construction on adjacent tunnels is critical. This study investigated the variation law of tunnel deformation and surrounding earth pressure on an existing tunnel resulting from deep foundation excavation and the load of buildings. Four groups of scale model tests and corresponding numerical simulation calculations were conducted in four different modes: over unloading-loading, shallow-side unloading-loading, middle-side unloading-loading, and deep-side unloading-loading, which are according to the different relative position of the foundation pit and the tunnel. The results show that when the tunnel stretches across different areas, corresponding deformation occurs owing to the different mechanical mechanisms during excavation and loading. The results can provide evidence for the further study on the impact of adjacent construction process on the tunnels.

1. Introduction

China has become the largest subway construction market, with subway construction currently at its peak in that market [1]. The convenience, speediness, and punctuality of subway networks have resulted in various city resources being built along subway lines. However, excavation of deep foundation pits and building construction result in a series of complex loading and unloading effects that change the stress and displacement fields of the soil surrounding adjacent tunnels. They also have an impact or even destroy the tunnel structure. Subway trains in service are quite sensitive to tunnel deformation—if a tunnel deformation is too large or if the structure is damaged, safe operation of subway trains is not guaranteed.

Numerous researchers have investigated the impact of adjacent construction on tunnels. Several [2–8] have studied the effect of excavation of new tunnels on existing tunnels. Others have examined the effect of foundation pit excavation. Zheng and Wei [9] studied the displacement of a tunnel and the change of the stress path of the soil surrounding the tunnel caused by excavation of a foundation pit at three different positions relative to the tunnel. Wang et al. [10] found that excavation causes an uneven uplifting of the shield tunnel below the foundation pit in the longitudinal direction through comparative study of numerical simulation and field measurement. Ng et al. [11] investigated the impact of sand density and retaining wall stiffness on the responses of a tunnel to pit excavation via a comparative study using the centrifuge simulation method and three-dimensional numerical simulation. Shi et al. [12] presented a simplified approximate method, developed via systematic study of numerical parameters, for evaluating the response of a tunnel under a foundation pit excavation. Beyabanaki and Gall [13] performed a three-dimensional numerical parametric study on the complex interaction between open-pit mining and an existing tunnel. Shi et al. [14] conducted a three-dimensional numerical parametric study that explored the complex interaction between basement excavation and a tunnel in dry sand. Chen et al. [15] investigated the effect of an adjacent large excavation on an existing tunnel of the Ningbo Metro Line 1 in soft soil. Zhang et al. [16] presented a semianalytical method to evaluate the displacement of tunnels induced by adjacent excavation.

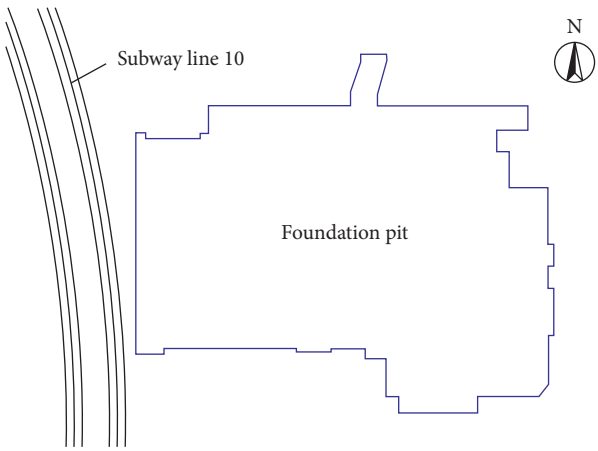

Figure 1: Plane position map of pit and tunnel.

Zhou et al. [17] proposed an analytic approach to predict and estimate the response of tunnels to adjacent foundation excavation.

However, only a few studies [18] have analyzed the impact of foundation pit excavation and loading in the pit on tunnel displacement and stress. Even fewer systematic studies aimed at the parameters relative to the spatial position between excavation, building, and tunnel have been conducted.

Based on a foundation pit being engineered near to an existing subway tunnel in eastern Beijing, in this study, four similar material simulation tests and corresponding numerical simulation calculations were carried out. More specifically, in this study, the impact of complex mechanical changes on tunnel deformation during the overall construction process of adjacent high-rise buildings was investigated.

2. Engineering Scenario and Loading-Unloading Mode

2.1. Engineering Scenario. The excavation project investigated in this study was carried out in Liangmaqiao Road, Chaoyang District, Beijing city. This is close to the west of the Sanyuanqiao-Liangmaqiao section of subway line 10, as shown in Figure 1. The outer diameter of the shield tunnel is 6.0 m, and the inner diameter is 5.4 m. The lining segment consists of C50 precast concrete segments, 0.3 m thick and 1.2 m wide. The lining segment is only 5.1 m away from the west of the project, and the excavation depth is 15 m. The support form is soil nailing wall on the top and diaphragm wall with prestressed anchor cable at the bottom. The basic parameters of the typical engineering strata are shown in Table 1.

2.2. Unloading-Loading Mode. Although many studies have been conducted in which the space between the tunnel and the foundation pit differs, as mentioned above, they are not related and difficult to compare owing to factors such as the supporting form of the foundation pit and the geological condition of the soil layer differing.

According to the different spatial positions between the foundation pit and the tunnel, this study classified four loading and unloading modes associated with the overall adjacent high-rise buildings construction process (as shown in Figure 2): over unloading-loading, shallow-side unloading-loading, middle-side unloading-loading, and deep-side unloading-loading. Further, the latter three modes are classified as side unloading-loading modes.

3. Model Test

3.1. Similarity Ratio. Considering the size of the model container, the accuracy of measuring apparatus, and other conditions, the ratio of geometric similarity was set as 15 : 1 and the ratio of unit weight similarity was 1 : 1. Equation (1) can be deduced from the equilibrium, geometric, and physical equations [19, 20].

The similarity ratio of dimensionless physical quantity is "1." When the dimensions of two parameters are the same, their similarity ratios are also the same. Then, the similarity ratios of the other material quantities can be deduced, as shown in Table 2:

$$\begin{aligned} C_\sigma &= C_\gamma C_{\mathrm{L}}, \\ C_\delta &= C_\varepsilon C_{\mathrm{L}}, \\ C_\sigma &= C_\varepsilon C_{\mathrm{E}}. \end{aligned} \tag{1}$$

3.2. Test Device and Similar Material. The test device was a large model test container composed of square splice plates, columns, ring beams, and so on, with dimensions 3000 mm × 1000 mm × 2000 mm.

The model soil was simulated using river sand and iron powder as the aggregate and lime and gypsum as adhesive. The materials proportion of each stratum is shown in Table 3. The anchor cable was simulated using wire rope and quick-dry cement. A portable electronic scale was used to stretch the anchor cable in the test.

3.3. Test Scheme. The support form was simplified as excavation with a slope on the top and diaphragm wall with prestressed anchor cable at the bottom. In-line with the four modes outlined above, four groups of tests were conducted. The layouts of the support structure are as shown in Figure 3.

The construction was simulated using the cast iron weights. In accordance with the national standard of China, the load of each floor was 12 kPa. Twelve weights were loaded onto the 0.8 m × 0.8 m mat foundation model each time.

Corresponding to the prototype, this is the load of two floors of construction. The layers of the load from Schemes 1–4 were as follows: 6, 6, 7, and 8.

3.4. Measuring Equipment. A guyed displacement sensor (range: 0–100 mm, accuracy: 0.01 mm) was applied to measure the displacement of the tunnel. The layout of the sensor is shown in Figures 2(a)–(d). The surrounding earth

Table 1: Basic parameters of the typical engineering strata.

Name	Cohesion (kPa)	Internal friction angle (°)	Unit weight (kN/m^3)	Compression modulus (MPa)	Poisson ratio	Thickness (m)
Miscellaneous fill	10	15.0	18.5	7.0	0.36	2.0
Clayey silt I	21	20.7	21.6	7.7	0.25	5.2
Silty clay	28.7	20.6	20.7	9.7	0.26	12.2
Clayey silt II	30	23.0	20.6	18.7	0.25	2.8
Medium sand	0	30.0	21.0	30.0	0.27	3.2
Pebbles	0	35.0	22.0	55.0	0.23	4.5

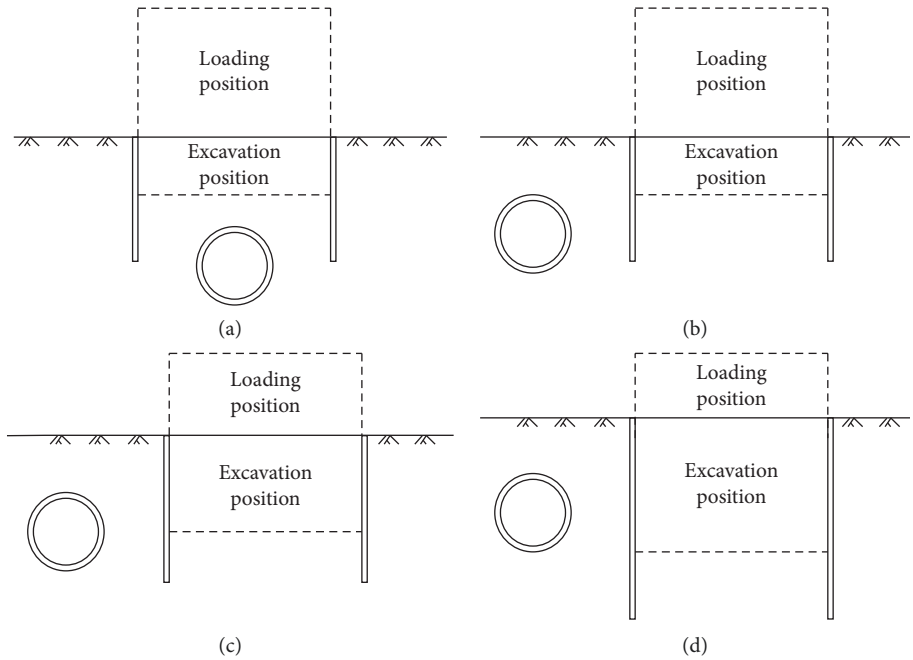

Figure 2: Unloading-loading modes associated with the adjacent high-rise buildings construction process. (a) Over unloading-loading mode. (b) Shallow-side unloading-loading mode. (c) Middle-side unloading-loading mode. (d) Deep-side unloading-loading mode.

Table 2: Similarity ratio of physical quantities of similar materials.

	Geometry, C_L	Displacement, C_δ	Elastic modulus, C_E	Cohesion, C_C	Stress, C_σ	Unit weight, C_γ	Internal friction angle, C_φ	Strain, C_ε	Poisson's ratio, C_μ
Ratio	15 : 1	15 : 1	15 : 1	15 : 1	15 : 1	1 : 1	1 : 1	1 : 1	1 : 1

pressure was measured using a miniature soil pressure cell (range: 100 kPa). Sixteen cells were set along the middle of the outer wall of the tunnel, as shown in Figure 4.

3.5. Model Test Conditions. The construction of the tunnel and the diaphragm wall were considered finished when the soil was laid in the container. Following completion of the preparatory work, the whole container remained static for more than 24 hours until all data were stable, after which the tests were conducted. Based on the test conditions of Scheme 3, as shown in Table 4, the conditions of the other test schemes were as follows. In Scheme 1, condition 8 was changed to "excavate to −600 mm depth." Subsequently, the container remained stationary. Finally, the container remained stationary after the sixth layer of weights was loaded. The conditions in Scheme 2 were the same as those in Scheme 1. In Scheme 4, condition 12 was changed to "excavate to −1066 mm depth." Then, conditions 13, 14, and 15 were added; specifically, "excavate to −1200 mm depth," "tension of the fourth layer of anchor cable completion,"

Table 3: Material proportion of each stratum.

Name	Ratio of material
Miscellaneous fill	Sand = 1
Clayey silt I	Sand : iron powder : lime : gypsum = 19 : 8 : 2 : 1
Silty clay	Sand : iron powder : lime : gypsum = 19 : 8 : 1 : 1
Clayey silt II	Sand : iron powder : lime : gypsum = 19 : 8 : 2 : 1
Medium sand	Sand = 1
Gravel pebbles	Sand : iron powder = 20 : 1

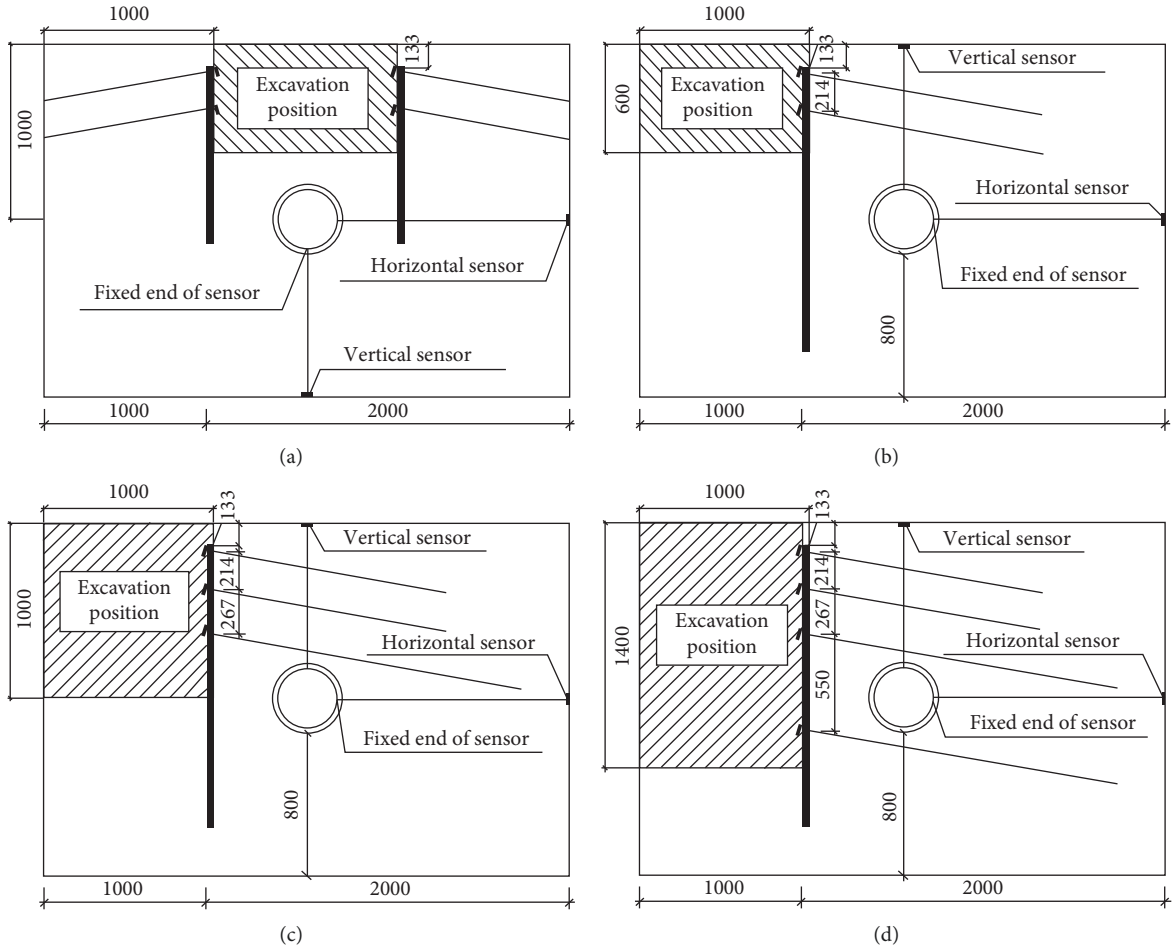

Figure 3: Layout of the support structure. (a) Scheme 1. (b) Scheme 2. (c) Scheme 3. (d) Scheme 4.

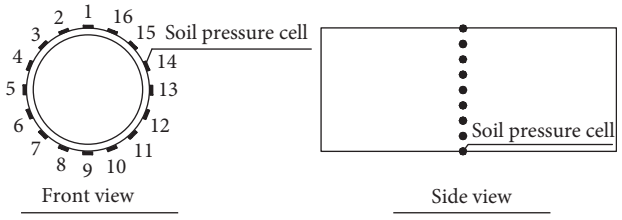

Figure 4: Layout of the measuring points.

and "excavate to −1400 mm depth," respectively. Subsequently, the container remained stationary. Finally, the container remained stationary after the eighth layer of weights was loaded.

3.6. Model Test Results and Analysis. In this paper, a positive vertical displacement value indicates that the tunnel is rising, whereas a negative value indicates that it is sinking. Further, a positive horizontal displacement value signifies tunnel movement toward the foundation pit, whereas a negative value signifies tunnel movement away from the foundation pit. Because the earth pressure cell can only measure pressure, it is always positive and signifies the cell being pressed. The black icons in Figure 5 indicate the completion of the foundation pit.

3.6.1. Tunnel Displacement Variation Law. In the excavation stages, there was a significant difference between Scheme 1 and the other three schemes, as shown in Figure 5. In contrast to the other schemes, the change in the vertical displacement was greater than that in the horizontal displacement for Scheme 1. When the tunnel is below the pit, it rises with the excavation procedure.

In Scheme 2, the tunnel slightly rises. With the excavation of the foundation pit, the state of the tunnel gradually changes from rising to sinking in Scheme 3. However, the tunnel maintains a rising state following completion of the excavation. In Scheme 4, the tunnel continues to sink following the displacement law of Scheme 3. The difference is that the tunnel is in a settlement state following completion of the excavation. In the horizontal direction, the tunnel moves to the foundation pit in the excavation stages in Schemes 2–4.

In the loading stages, the tunnel sinks in all schemes. In Scheme 1, there is virtually no horizontal displacement of the tunnel. In Scheme 2, the tunnel has horizontal

Table 4: Model test conditions for Scheme 3.

Condition number	Condition description
1	Read initial value
2	Excavate to −133 mm depth
3	Tension of the first layer of anchor cable
4	Excavate to −266 mm depth
5	Excavate to −400 mm depth
6	Tension of the second layer of anchor cable
7	Excavate to −533 mm depth
8	Excavate to −666 mm depth
9	Tension of the third layer of anchor cable
10	Excavate to −800 mm depth
11	Excavate to −933 mm depth
12	Excavate to −1000 mm depth
13	Remain stationary after excavation completion
14	Load the mat foundation
15	Load first layer of weights
16	Load second layer of weights
17	Load third layer of weights
18	Load fourth layer of weights
19	Load fifth layer of weights
20	Load sixth layer of weights
21	Load seventh layer of weights
22	Remain stationary after loading completion

displacement away from the foundation pit. In Schemes 3 and 4, the tunnel slightly moves towards the pit.

3.6.2. Variation Law of the Surrounding Earth Pressure on the Tunnel. As shown in Figure 6, the surrounding earth pressures on the tunnel at the top and bottom are much larger than those on the lateral sides.

In Scheme 1, following excavation, because of the release of the earth pressure, the surrounding earth pressure on the tunnel significantly decreases. The decrease in the pressures at the top and bottom is greater than that for the lateral sides. When the construction loads, the pressures significantly increase. However, they are less than their initial values because the total load is less than the initial soil load. In Schemes 2–4, the distribution law and change tendency are the same as those in Scheme 1. However, the extent of change is much less. The main reason is the different spatial position. In addition, the distance between the tunnel and the pit is much less than in Scheme 1.

4. Numerical Simulation Analysis

In accordance with the physical simulation schemes, four groups of numerical simulation tests were conducted. The three-dimensional finite difference simulation software FLAC3D was utilized.

4.1. Calculation Model and Scheme. The calculation range of the model was $X = 120$ m, $Y = 160$ m, and $Z = 60$ m. The speed of the three directions of the bottom boundary nodes and the speed of the horizontal directions of the lateral boundary nodes were constrained. In the model, the solid

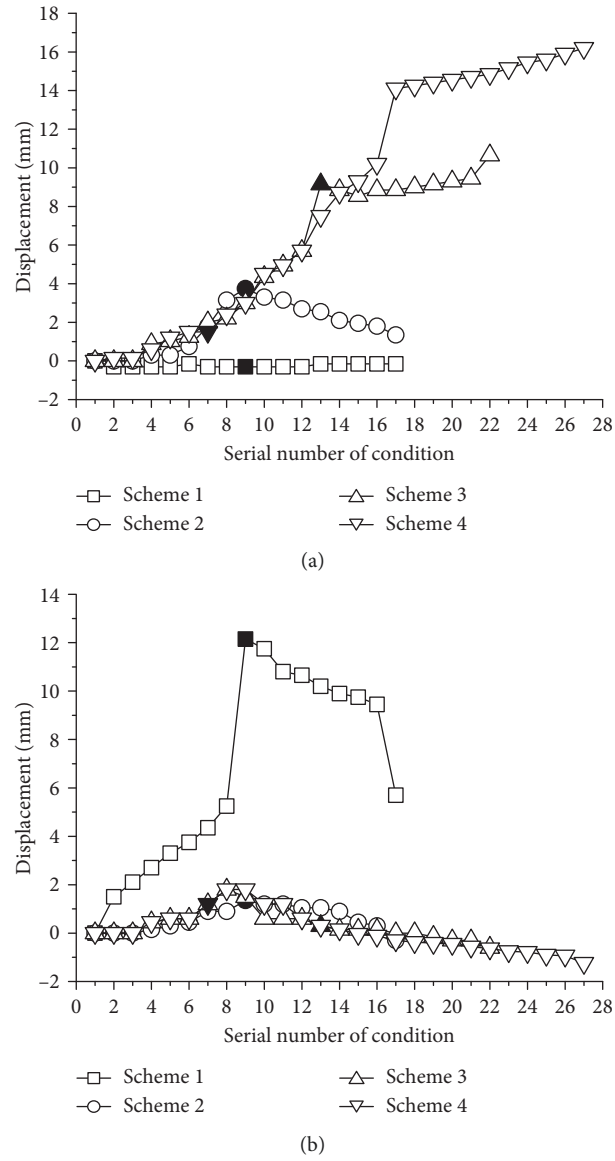

Figure 5: Time history diagram of displacement of the tunnel. (a) Horizontal displacement. (b) Vertical displacement.

element was used for soil, diaphragm wall, and tunnel. The cable element of FLAC3D was used for the anchor bolt.

The calculation models corresponded with the physical simulation, using the prototype size. The meshing of the model grid unit is shown in Figure 7. The relative position of the pit support structure and the tunnel are shown in Figure 8. The layout of the measuring point is in agreement with the model test.

4.2. Model Parameter Selection. Studies [21–24] have shown that the soil hardening model is more appropriate for simulating the deformation of the surrounding soil caused by foundation pit excavation. It can take into account the plasticity of clay and strain hardening characteristics and can distinguish the difference between loading and unloading, and the stiffness depends on the stress level. Thus, the modified Cam-Clay

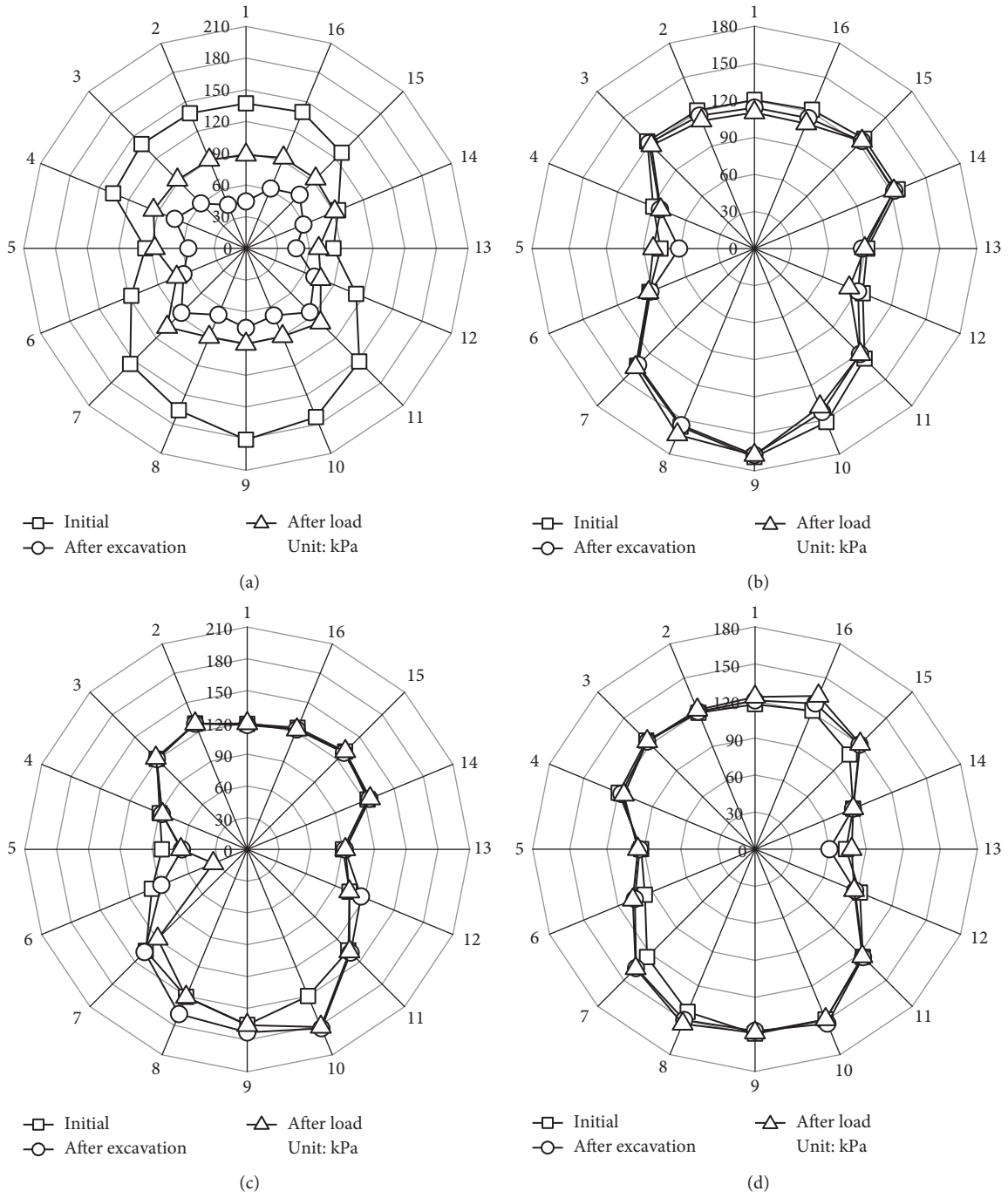

Figure 6: Surrounding earth pressure on the tunnel. (a) Scheme 1. (b) Scheme 2. (c) Scheme 3. (d) Scheme 4.

(MCC) model was chosen as the constitutive soil model in this paper. The diaphragm wall, mat foundation, building, tunnel, and anchor cable applied the elastic model.

The main parameters in the modified Cam-Clay model were the slope of the normal consolidation curve λ, the slope of the swelling line κ, the slope of the critical state line M, Poisson's ratio ν, and elastic modulus E. The main parameters of the soil layers were based on the geological survey, the existing engineering experience in the Beijing area, and (2). There were six layers of soil in the depth range. The parameters of the soil in the modified Cam-Clay model are shown in Table 5. The parameters of the support structure are shown in Table 6.

$$\lambda = \frac{C_c}{\ln 10},$$
$$\kappa = \frac{C_s}{\ln 10}, \tag{2}$$
$$M = \frac{6 \sin \varphi'}{3 - \sin \varphi'},$$

where C_c = compression index, C_s = rebound index, and φ' = effective internal friction angle.

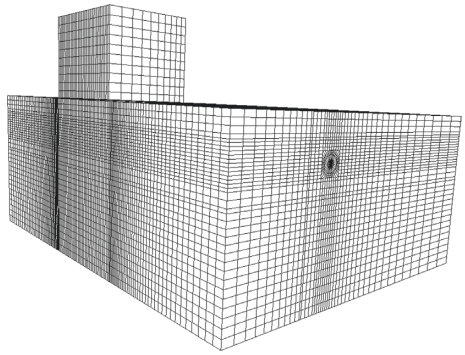

Figure 7: Meshing of the model grid unit.

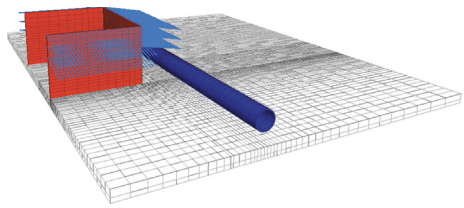

Figure 8: Meshing of the support structure and tunnel.

Table 5: Main parameters of each stratum.

Parameter number	Slope of critical state line, M	Slope of the normal consolidation line, λ	Slope of the swelling line, κ
1	0.4	0.09	0.003
2	1.02	0.09	0.004
3	2.05	0.07	0.002
4	1.24	0.09	0.004
5	1.42	0.02	0.001
6	1.42	0.01	0.001

4.3. Numerical Simulation Results and Analysis. The locations of the measurement points of the surrounding earth pressure were the same as those in the model test. The displacement of each of the points was also analyzed. The regulations of positive and negative values were the same as those in the physical simulation tests. The numerical simulation conditions for Scheme 3 are shown in Table 7. The conditions for the other schemes corresponded to those applied in the model test. The black icons in Figures 9–12 indicate the completion of the foundation pit. This study investigated the middle section of the tunnel. This section mainly discusses the deformation law of the tunnel. The mechanical mechanism of deformation is discussed in Section 4.5.

4.3.1. Tunnel Displacement Variation Law. In general, the vertical displacement of the tunnel was much greater than the horizontal displacement in Scheme 1. In the other schemes, with increasing excavation depth, the vertical displacement of the tunnel gradually changed from slightly smaller than horizontal displacement to much less than the horizontal displacement.

(1) Change Law of Vertical Displacement of the Tunnel. In Scheme 1, in the excavation stage, in addition to the global displacement trend, the tunnel structure gradually produced vertical tension and horizontal extrusion. With the increase of unloading of the soil, the difference in the upper and the lower displacement and the horizontal convergence increased. In contrast, these two decreased as the load increased. Finally, the tunnel was still in a state of tension in the vertical direction and compaction in the horizontal direction compared to its initial state, as shown in Figure 9.

In Scheme 2, in the excavation stage, the tunnel rose. Simultaneously, according to the vertical displacement difference between measuring points 5 and 13, and the horizontal displacement difference between measuring points 1 and 9, it can be judged that the tunnel started to turn clockwise. After the loading of the building, uneven settlement of soil under the tunnel led to anticlockwise rotation of the tunnel, as shown in Figure 10.

In Scheme 3, with the increase in the depth of the excavation, the tunnel gradually shifted from the rising state to the sinking state and rotated anticlockwise. After the excavation, it was still in the rising state. In Scheme 4, the tunnel kept sinking after the same condition as that in Scheme 3 and maintained the sinking state after the end of the excavation. In the loading stage, the variation law of the tunnel displacement in Schemes 3 and 4 is similar to that in Scheme 2, as shown in Figure 11.

(2) Change Law of Horizontal Displacement of the Tunnel. The variation law of the horizontal displacement was consistent with that in the physical simulation test. However, the building in the numerical simulation was tightly connected to the wall and had a certain stiffness, which can resist the deformation of the diaphragm wall. Therefore, in Scheme 4, in the loading stage, the tunnel moved slightly towards the foundation pit because of the anticlockwise rotation of the tunnel, which is different from the physical simulation.

4.3.2. Variation Law of Surrounding Earth Pressure on the Tunnel. The distribution and variation of the surrounding earth pressure on the tunnel in numerical simulation were similar to those for the physical simulation. On the whole, it had an elliptical distribution with major axis in the vertical direction.

As shown in Figure 13, the vertical unloading of earth pressure on the tunnel was obviously greater than the horizontal unloading in Scheme 1. However, it was the opposite in Schemes 2–4. Further, along with the gradual increase of tunnel burial depth relative to the foundation pit, unloading was gradually reduced. However, it was the opposite in the loading stages. Further, the change of surrounding earth pressure on the tunnel was uneven. These change law corresponded to the characteristics of tunnel displacement response discussed in the previous section.

4.4. Comparison between Physical Simulation and Numerical Simulation. In the physical simulation, the similarity ratio is an important value. The value shown in Table 2 is the

Table 6: Main parameters of the support structure.

Parameter name	Elastic modulus, E (MPa)	Poisson's ratio, ν	Unit weight (kN/m^3)
Diaphragm wall	$3.15E+4$	0.2	25
Lining segment	$3.45E+4$	0.2	25
Mat foundation	$3.15E+4$	0.2	25
Anchor wire	$2.10E+5$	0.2	78

theoretical value of the similarity ratio of each physical parameter. The internal friction angle, cohesion, and elastic modulus were the main reference values while making the test materials. Because of the restricting test conditions, when the similarity ratios of the three factors above are equal to the theoretical values, the severe similarity ratios cannot be completely equal to the theoretical values at the same time. Therefore, the model test is mainly the qualitative analysis, and there is some difference between the values in the physical simulation and the numerical simulation. However, in general, the results of the numerical simulation are similar to the basic rules of the results of the physical model tests. These results can verify their consistency.

4.5. Mechanical Mechanism of Tunnel Deformation. The mechanical mechanism of the deformation of the tunnel can be summed up in light of the comparison and analysis of the physical and numerical simulation results.

4.5.1. Mechanical Mechanism in over Unloading-Loading Mode. When the foundation pit is excavated, the soil under the foundation pit is horizontal and vertical unloading at the same time, as shown in Figure 13. The soil rebounds because of the unloading. Further, under the bottom of the pit, the earth pressure on both sides of the diaphragm wall is obviously unbalanced. This makes the soil outside the diaphragm wall move towards the pit, and it also compresses the soil in the pit and produces vertical deformation. The tunnel rises upward under the combined influence of these two factors.

Simultaneously, as shown in Figure 13, as the vertical unloading is greater than the horizontal unloading and the lateral extrusion of the soil outside the pit, the tunnel undergoes vertical tension and horizontal convergence in addition to the global movement.

When the building is loaded into the pit, the building load produces additional base stress on the underlying soil. The soil beneath the tunnel is consolidated and compressed as a result of the additional base stress, and it results in the tunnel settlement.

Further, as shown in Figure 13, as the vertical loading is greater than the horizontal loading, the tunnel undergoes vertical convergence and horizontal tension in addition to the global movement.

4.5.2. Mechanical Mechanism in Side Unloading-Loading Mode. When the foundation pit is excavated, the earth pressure on the outer side of the foundation pit changes from static earth pressure to active earth pressure. It is horizontal unloading, and the unloading amount decreases with increasing distance from the diaphragm wall. Therefore, the tunnel in the shallow area outside of the foundation pit moves towards the pit because of the difference in the earth pressure on the horizontal sides. As shown in Figure 13, when the tunnel is in the shallow area outside of the foundation pit, the change in the surrounding earth pressure is the largest. In addition to the global displacement and rotation, the tunnel may also cause structural deformation. Further, when the tunnel is in the deep area outside of the foundation pit, the change in the surrounding earth pressure is the smallest. The deformation of the tunnel structure is very small.

The diaphragm wall also moves towards the foundation pit, which causes ground loss and forms a settlement trough from the surface. The settlement value decreases with the increase in the depth, and the settlement range increases with the increase in the excavation depth. When the tunnel is in the settlement trough, it sinks with the soil.

At the same time, the diaphragm wall rises owing to the rebound of the soil at the bottom of the foundation pit, leading the deep soil to float slightly together. In the horizontal direction, the earth pressure on both sides of the diaphragm wall is unbalanced, and the soil moves towards the foundation pit. Therefore, the tunnel in the deep position out of the pit moves along with the soil towards the foundation pit, including horizontal or vertical.

Table 7: Numerical simulation conditions for Scheme 3.

Condition number	Condition description
1	Initial stress state, clear displacement field
2	Completion of shield tunnel, clear displacement field
3	Excavate to −2.0 m depth
4	Completion of the first layer of anchor cable
5	Excavate to −4.0 m depth
6	Excavate to −6.0 m depth
7	Completion of the second layer of anchor cable
8	Excavate to −8.0 m depth
9	Excavate to −10.0 m depth
10	Completion of the third layer of anchor cable
11	Excavate to −12.0 m depth
12	Excavate to −14.0 m depth
13	Excavate to 15.0 m depth
14	Completion of mat foundation
15	Completion of basement floors −4 and −3
16	Completion of basement floors −2 and −1
17	Completion of building floors 1 and 2
18	Completion of building floors 3 and 4
19	Completion of building floors 5 and 6
20	Completion of building floors 7 and 8
21	Completion of building floors 9 and 10

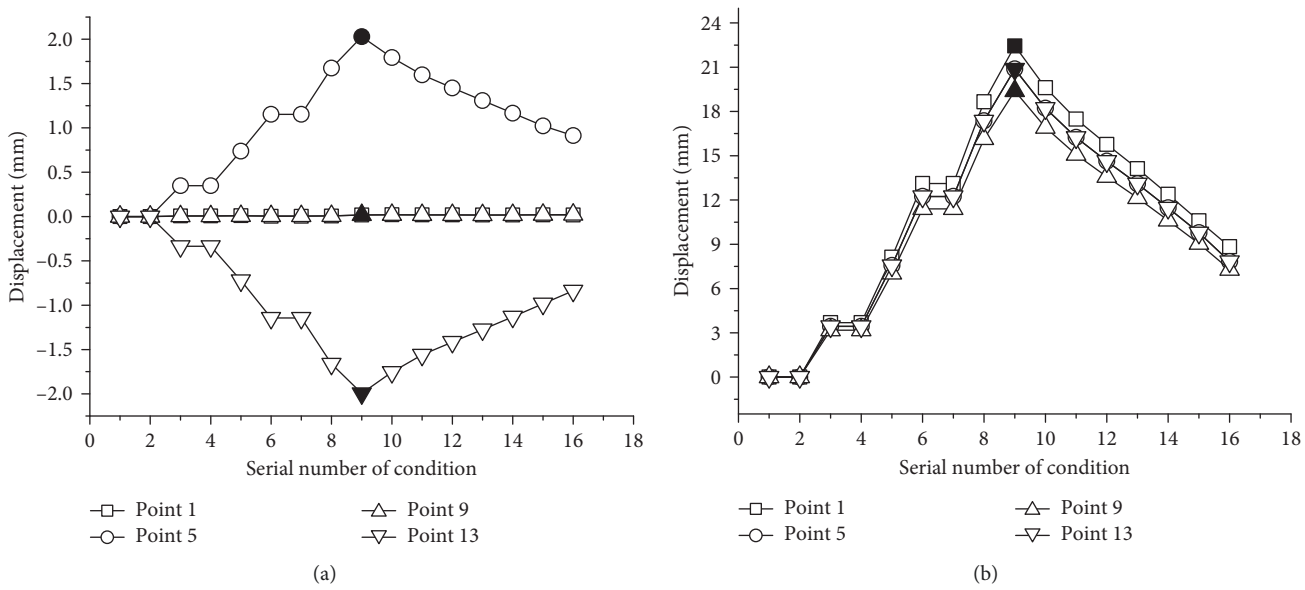

Figure 9: Time history of displacement of the tunnel in Scheme 1. (a) Horizontal displacement. (b) Vertical displacement.

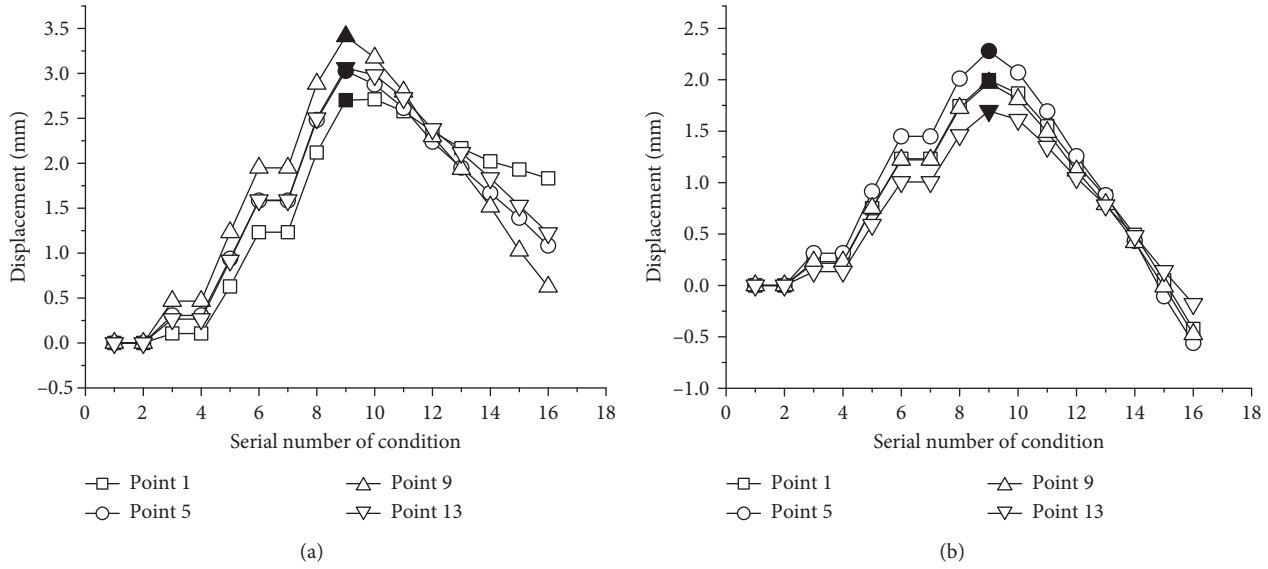

Figure 10: Time history of displacement of the tunnel in Scheme 2. (a) Horizontal displacement. (b) Vertical displacement.

When the foundation pit is excavated, the displacement field outside the pit is uneven. Therefore, the tunnel rotates in addition to the global movement. Thus, the direction of rotation varies with the vertical position of the tunnel.

When the building is loaded, the additional base stress spreads around, but it is not uniform. Therefore, the lateral part of the foundation pit produces uneven consolidation compression, and the tunnel rotates in addition to the global settlement.

The additional base stress also produces additional lateral stress that pushes the soil away from the foundation pit and produces thrust to the bottom of the diaphragm wall. Then, the tunnel in the deeper section outside of the foundation pit moves away from the pit. However, this effect mainly affects the tunnel in the deep area outside of the pit and has little effect on the tunnel in the shallow area outside of the pit.

Therefore, when the tunnel stretches across different areas, corresponding deformation occurs owing to the different mechanical mechanisms during excavation and loading. The tunnel presents different deformation laws in Schemes 1–4, respectively.

5. Conclusions

To investigate different spatial positions in relation to the foundation pit, the building, and the tunnel, in this study, four groups of large-scale physical simulation tests and corresponding numerical simulation calculations were designed and implemented. In this paper, the deformation

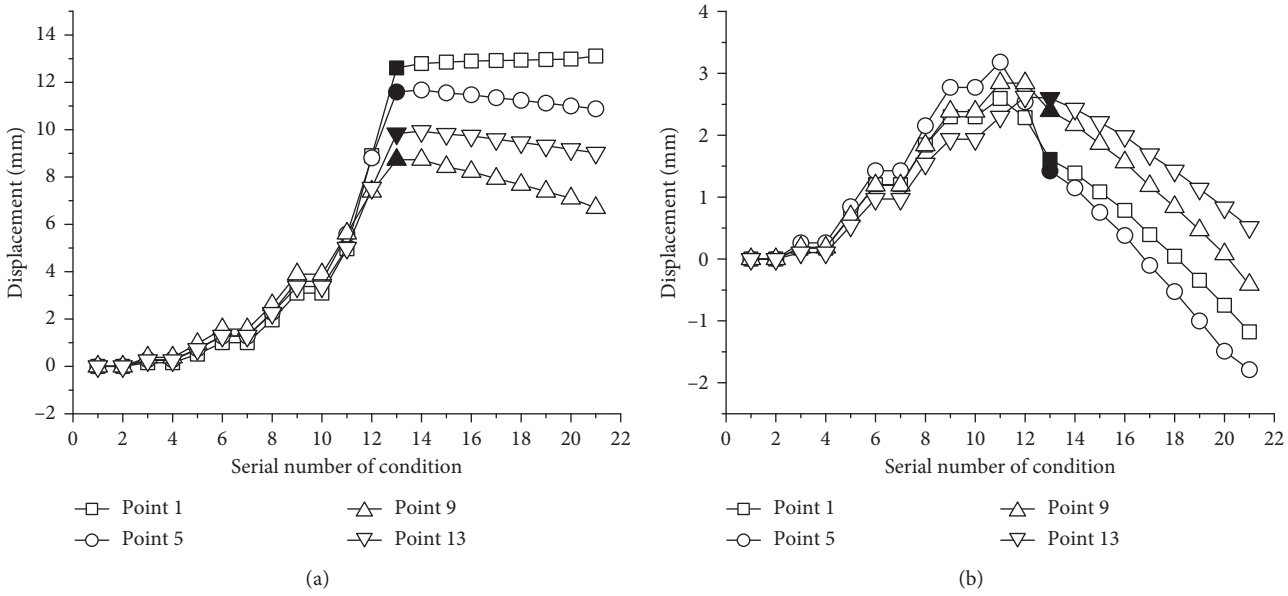

Figure 11: Time history of displacement of the tunnel in Scheme 3. (a) Horizontal displacement. (b) Vertical displacement.

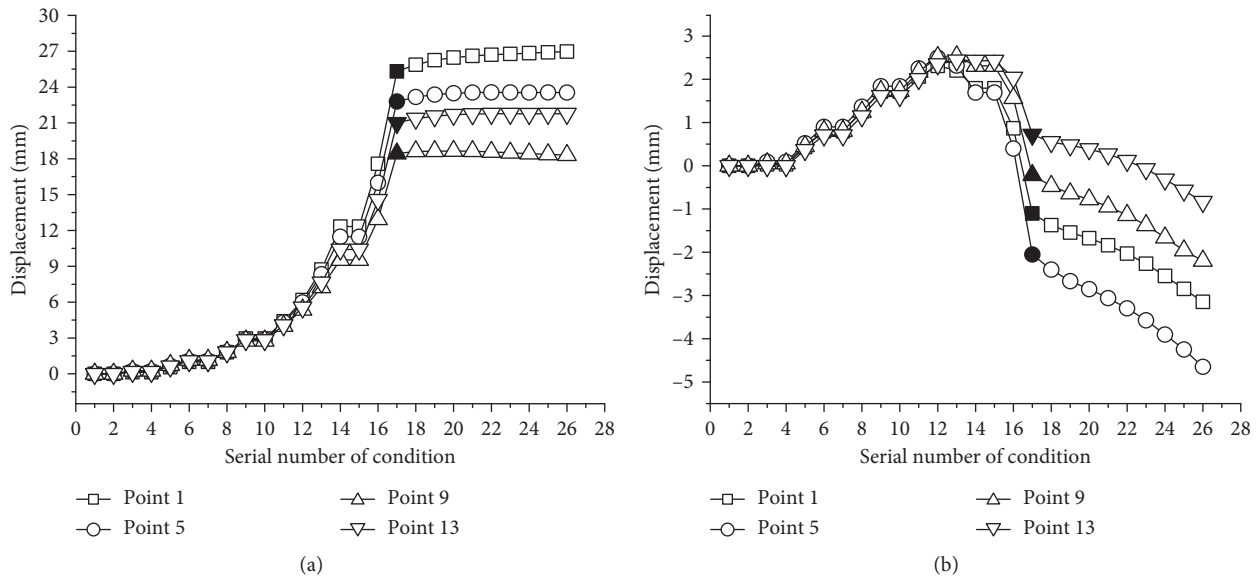

Figure 12: Time history of displacement of the tunnel in Scheme 4. (a) Horizontal displacement. (b) Vertical displacement.

characteristics, the distribution law of surrounding earth pressure of the subway tunnel, and their mechanical mechanism under different modes were presented. The results presented have theoretical significance for future construction:

(1) The amount of unloading and loading and their relative positions in relation to the tunnel are critical factors of the different variations of the surrounding soil pressure and displacement of the tunnel.

(2) The vertical unloading of earth pressure on the tunnel was obviously greater than the horizontal unloading in the over unloading-loading mode. However, it was the opposite in the side unloading-loading mode.

(3) In the excavation stage, the tunnel moves towards the foundation pit owing to the unloading-rebound effect and the unbalanced horizontal earth pressure. In the side unloading-loading mode, the tunnel rotates towards to the foundation pit. In the over unloading-loading mode, the tunnel has obvious self-deformation.

(4) In the loading stage, the tunnel sinks gradually in each mode owing to the spread of the additional base stress. In the horizontal direction, the tunnel moves away from the foundation pit under the shallow lateral mode and towards the pit under the other side modes.

(5) In the side unloading-loading mode, the horizontal displacement is larger than the vertical displacement

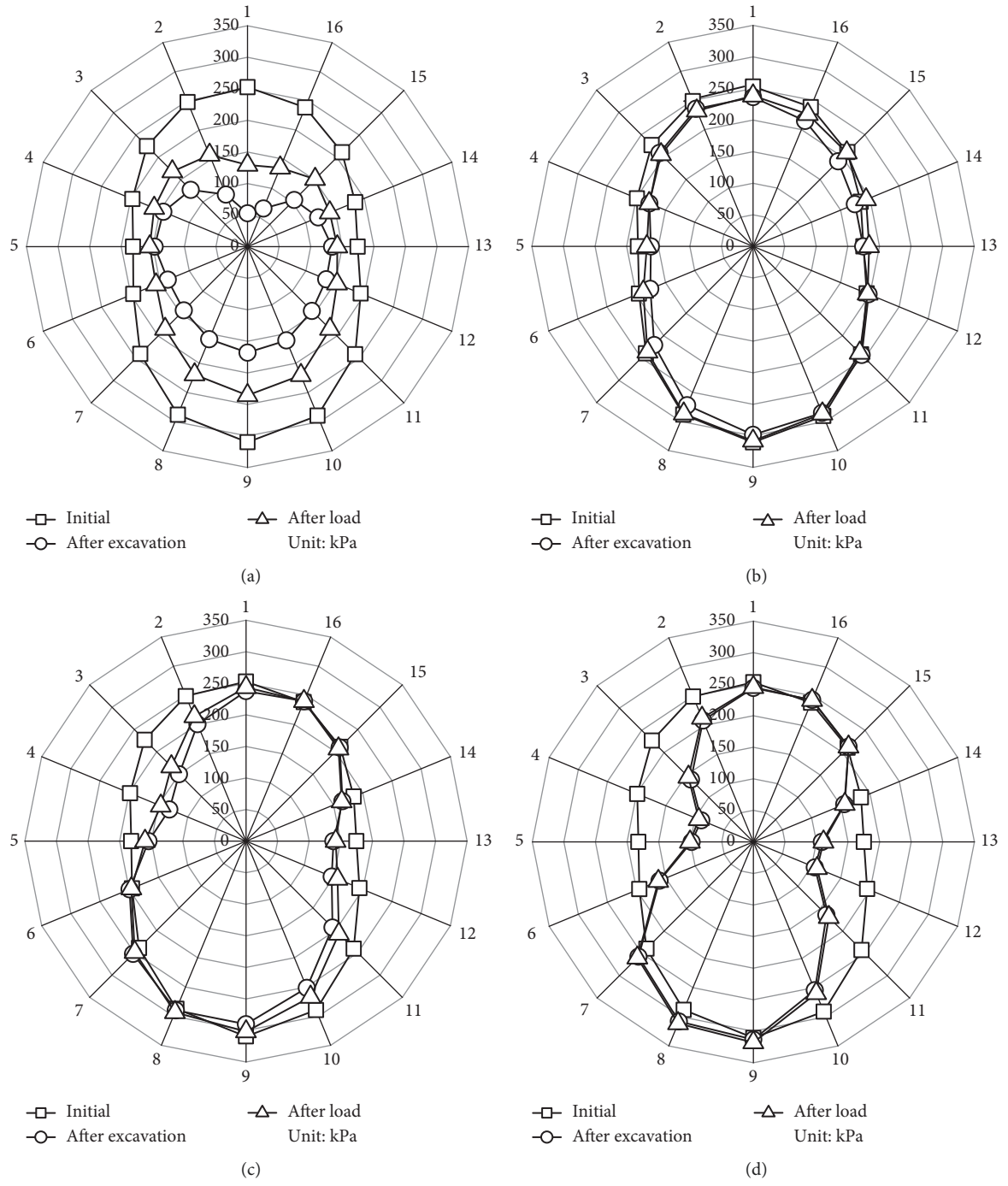

Figure 13: Radar diagram of the surrounding earth pressure on the tunnel. (a) Scheme 1. (b) Scheme 2. (c) Scheme 3. (d) Scheme 4.

of the tunnel, and it is the opposite in the over unloading-loading mode. Therefore, in engineering, the horizontal displacement of the tunnel in the side unloading-loading mode and vertical displacement of the tunnel in the over unloading-loading mode should be controlled.

(6) This paper simplifies the field conditions and ignores the impact of groundwater. However, in practical engineering, the groundwater is an important factor to influence the safety of the structure. Further work needs to consider the impacts of groundwater.

Data Availability

The data used to support the findings of this study are available from the corresponding author upon request.

Conflicts of Interest

The authors declare that they have no conflicts of interest.

Acknowledgments

The authors appreciate the support from the National Natural Science Foundation of China (No. 51578023). The authors would like to thank Editage (www.editage.com) for English language editing.

References

[1] H. W. Huang, "State-of-the-art of the research on risk management in construction of tunnel and underground works," *Chinese Journal of Underground Space and Engineering*, vol. 2, pp. 13–20, 2006.

[2] H. B. Yun, S. H. Park, N. Mehdawi et al., "Monitoring for close proximity tunneling effects on an existing tunnel using principal component analysis technique with limited sensor data," *Tunnelling and Underground Space Technology*, vol. 43, pp. 398–412, 2014.

[3] Z. G. Zhang and M. S. Huang, "Geotechnical influence on existing subway tunnels induced by multiline tunneling in Shanghai soft soil," *Computers and Geotechnics*, vol. 56, pp. 121–132, 2014.

[4] J. R. Standing, D. M. Potts, R. Vollum et al., "Research into the effect of tunneling on existing tunnels," *Geotechnical Engineering for Infrastructure and Development*, vol. 2, pp. 301–312, 2015.

[5] H. L. Liu, P. Li, and J. Y. Liu, "Numerical investigation of underlying tunnel heave during a new tunnel construction," *Tunnelling and Underground Space Technology*, vol. 26, no. 2, pp. 276–283, 2011.

[6] Q. Fang, D. L. Zhang, Q. Q. Li, L. Ngai, and Y. Wong, "Effects of twin tunnels construction beneath existing shield-driven twin tunnels," *Tunnelling and Underground Space Technology*, vol. 45, pp. 128–137, 2015.

[7] X. G. Li and D. J. Yuan, "Response of a double-decked metro tunnel to shield driving of twin closely under-crossing tunnels," *Tunnelling and Underground Space Technology*, vol. 28, pp. 18–30, 2012.

[8] D. L. Jin, D. J. Yuan, X. G. Li, and H. Zheng, "An in-tunnel grouting protection method for excavating twin tunnels beneath an existing tunnel," *Tunnelling and Underground Space Technology*, vol. 71, pp. 27–35, 2018.

[9] G. Zheng and S. W. Wei, "Numerical analyses of influence of overlying pit excavation on existing tunnels," *Journal of Central South University of Technology*, vol. 15, no. 2, pp. 69–75, 2008.

[10] F. Wang, D. M. Zhang, H. H. Zhu, and J. H. Yin, "Impact of overhead excavation on an existing shield tunnel: field monitoring and a full 3D finite element analysis," *Computers Materials and Continua*, vol. 34, no. 1, pp. 63–81, 2013.

[11] C. W. W. Ng, J. Shi, D. Mašín, H. Sun, and G. H. Lei, "Influence of sand density and retaining wall stiffness on three-dimensional responses of tunnel to basement excavation," *Canadian Geotechnical Journal*, vol. 52, pp. 1811–1829, 2015.

[12] J. W. Shi, C. W. W. Ng, and Y. H. Chen, "A simplified method to estimate three-dimensional tunnel responses to basement excavation," *Tunnelling and Underground Space Technology*, vol. 62, pp. 53–63, 2017.

[13] A. R. Beyabanaki and V. Gall, "3D numerical parametric study of the influence of open-pit mining sequence on existing tunnels," *International Journal of Mining Science and Technology*, vol. 27, pp. 459–466, 2017.

[14] J. W. Shi, C. W. W. Ng, and Y. H. Chen, "Three-dimensional numerical parametric study of the influence of basement excavation on existing tunnel," *Computers and Geotechnics*, vol. 63, pp. 146–158, 2015.

[15] R. P. Chen, F. Y. Meng, Z. C. Li, Y. Ye, and J. Ye, "Investigation of response of metro tunnels due to adjacent large excavation and protective measures in soft soils," *Tunnelling and Underground Space Technology*, vol. 58, pp. 224–235, 2016.

[16] J. F. Zhang, J. J. Chen, J. H. Wang, and Y. F. Zhu, "Prediction of tunnel displacement induced by adjacent excavation in soft soil," *Tunnelling and Underground Space Technology*, vol. 36, pp. 24–33, 2013.

[17] Z. Zhou, S. Chen, P. Tu, and H. Zhang, "An analytic study on the deflection of subway tunnel due to adjacent excavation of foundation pit," *Journal of Modern Transportation*, vol. 23, no. 4, pp. 287–297, 2015.

[18] M. Dolezalova, "Tunnel complex unloaded by a deep excavation," *Computers and Geotechnics*, vol. 28, no. 6-7, pp. 469–493, 2001.

[19] E. Fumagalli, *Statical and Geomechanical Models*, Springer, New York, NY, USA, 1973.

[20] J. Wang, Y. Deng, R. Ma et al., "Model test on partial expansion in stratified subsidence during foundation pit dewatering," *Journal of Hydrology*, vol. 557, pp. 489–508, 2018.

[21] Z. H. Xu and W. D. Wang, "Selection of soil constitutive models for numerical analysis of deep excavations in close proximity to sensitive properties," *Rock and Soil Mechanics*, vol. 31, pp. 258–264, 2010.

[22] Z. H. Xu, *Deformation Behavior of Deep Excavations Supported by Permanent Structure in Shanghai Soft Deposit*, Shanghai JIAO TONG University, Shanghai, China, 2007.

[23] W. D. Wang, H. R. Wang, and Z. H. Xu, "Experimental study of parameters of hardening soil model for numerical analysis of excavations of foundation pits," *Rock and Soil Mechanics*, vol. 33, pp. 2283–2290, 2012.

[24] E. Zhou, *Application of Hardening Soil Model with Small-Strain in Deformation Analysis for Foundation Pit*, Harbin Institute of Technology, Harbin, China, 2010.